AD-A129 051 DIFAR-LIKE TRACKING ANOMALY STUDY THEORETICAL 1/1
PERFORMANCE COMPARISON: CLO..(U) RAYTHEON CO PORTSMOUTH
RI SUBMARINE SIGNAL DIV J F BARTRAM NOV 81 R2291
UNCLASSIFIED N00140-78-G-6021 F/G 17/3 NL

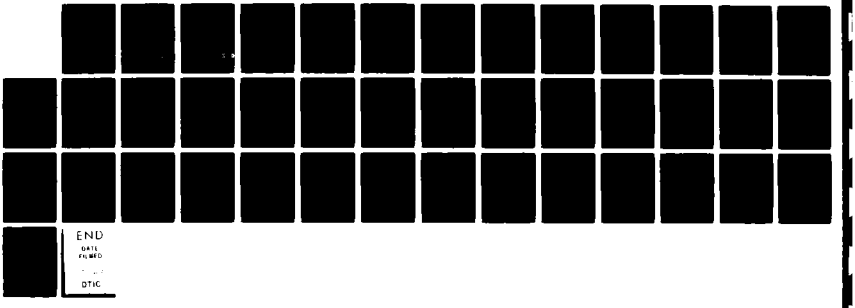

END
DATE FILMED
DTIC

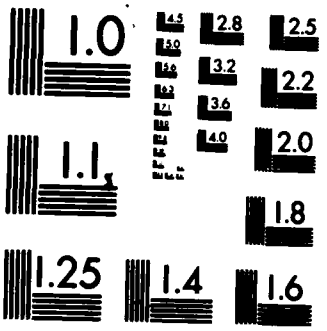

MICROCOPY RESOLUTION TEST CHART
NATIONAL BUREAU OF STANDARDS-1963-A

TECHNICAL REPORT
DIFAR-LIKE TRACKING
ANOMALY STUDY

Theoretical Performance Comparison:
Closed- vs Open-Loop Bearing Estimation,
Using Phase

Contract N00140-78-6021-0052

RAYTHEON COMPANY
SUBMARINE SIGNAL DIVISION
RAYTHEON

R2291

TECHNICAL REPORT
DIFAR-LIKE TRACKING
ANOMALY STUDY

Theoretical Performance Comparison: Closed- vs Open-Loop Bearing Estimation, Using Phase

by

James F. Bartram

Prepared for

U.S. Navy Underwater Systems Center

Under Contract N00140-78-G-6021-0052

November 1981

RAYTHEON COMPANY

SUBMARINE SIGNAL DIVISION

Portsmouth, Rhode Island 02871

TABLE OF CONTENTS

LIST OF ILLUSTRATIONS

ABSTRACT

Two basic approaches to the problem of estimating bearing in the ocean are compared. These approaches, both of which utilize signal phase, rather than amplitude, information, are the traditional closed-loop method and a newer open-loop concept. The relative theoretical performance is determined in terms of the standard deviation of fluctuation in the bearing estimate, normalized for universality. Bias considerations are neglected for simplicity. When the resulting closed- and open-loop performance curves are compared, it is found that there is little difference between them at high signal-to-noise ratios.

HIGHLIGHTS OF REPORT

- Bearing information imbedded in differential signal phase is identified.
- Basic configurations of closed-loop and open-loop bearing estimators used in the study are defined.
- The phase detection functions, although different in appearance, prove to be mathematically identical.
- Phase statistics are derived.
- The location and nature of the error differ significantly between the two estimators.
- Performance of the two estimators is evaluated and compared.
- The theoretical performance of the two estimators is the same at high signal-to-noise ratios.
- The decision as to which estimator to choose should be based on considerations other than theoretical performance.

RECOMMENDATIONS FOR FUTURE STUDY

- This study has made several simplifying assumptions:
  - No source motion
  - Source exactly on beam main response axis
  - Noise in the two half beams statistically independent of each other.

  A more realistic comparison would result if these assumptions were to be relaxed. This is recommended for a future study task or combination of tasks.

- This study has examined the use of signal phase to estimate bearing. It is recommended that a similar study be initiated to examine the use of signal amplitude instead: fundamentally, the performance of a bearing interpolation scheme. Other studies of this type have been performed, but not necessarily asking the questions that need to be asked for this application.

1.0 INTRODUCTION

This is a technical report prepared under the "DLT Anomaly Study" performed by the author under the technical direction of Peter J. Barnikel, NUSC/NLL, under contract N00140-78-6021-0052.

The question addressed in the present report is the following: Is there a fundamental difference in theoretical performance between a closed-loop bearing estimator, typified by the DIFAR-Like Tracker (DLT)[1], on the one hand, and an open-loop bearing estimator on the other hand, both estimators making use of signal phase, rather than amplitude, information?

It should be mentioned in passing at this point that studies[2-4] have been performed on the subject of bearing estimation (interpolation) using amplitude information. Despite this, it would be wise to perform such a study in the future, asking and answering the right questions pertinent to the application at hand. In particular, performance should be compared with the performance results obtained in the present report.

This report is quite theoretical, making many simplifying assumptions and working with normalized quantities to arrive at a performance comparison between idealized classes of systems. At no time is any information on the absolute performance of any real system derived or provided; that would be beyond the scope of the present study.

Since the bearing estimators under consideration use phase information, the second section of this report is devoted to an examination of the information carried in signal phase. The third section shows the basic configurations of the closed-loop and open-loop bearing estimators under study in this report. The fourth section analyzes the respective phase detection implementations. The fifth section presents the phase statistics derived in Appendix A. The sixth section examines the location and nature of the error in the two estimators. Finally, the performance of the estimators is evaluated and compared in the seventh section.

---

1. References are listed in Section 8.

2.0 PHASE INFORMATION

The two bearing estimation concepts being compared in this report both make use of information contained in the phase of the arriving signal. In this section, the information content of the signal phase is examined.

First, the signal is described: It will be assumed in this report that the signal waveform is a pure sinusoid and that the signal wavefront is plane. That is, the radiating source is assumed to be in the far field and the propagation is assumed to be ideal, introducing no multipath structure and no fluctuation, either in amplitude or in phase. In general, relative motion can exist and have an effect; in the end, however, relative motion will be assumed not to exist.

Second, the receiving array is described: For both bearing estimation concepts, an array of hydrophones split into left and right halves is used. The baseline distance between phase centers of these halves is called the effective dipole spacing (d).

The signals appearing in the left- and right-half beam outputs can be written as follows:

$$S_L(t) = A \cos \left[2\pi f_0 t + \Phi_L(t)\right] \tag{2-1}$$

$$S_R(t) = A \cos \left[2\pi f_0 t + \Phi_R(t)\right] \tag{2-2}$$

where

A = constant signal amplitude, usually the same in both half beams (although not a requirement),

f_0 = source frequency of signal,

$\Phi_{L,R}$ = phase terms in left and right half beams respectively, further described as follows:

$$\Phi_{L,R} = \kappa \left\{ -r_i(t) \pm \frac{d}{2} \left[\sin \theta_i(t) - \sin \theta_o \right] \right\} + \Phi_0 \qquad (2\text{-}3)$$

where κ = acoustic wave number:

$$\kappa = \frac{2\pi}{\lambda} = \frac{2\pi f_0}{c} \qquad (2\text{-}4)$$

where

λ = acoustic wavelength
c = speed of sound

Continuing,

r_i = range to source
θ_i = bearing to source
θ_o = bearing direction of array main response axis (MRA)
Φ_0 = constant additive phase shift.

Now the information contained in the phase terms given by (2-3) will be discussed. To start, the constant additive phase shift (Φ_0), of course, conveys no information at all.

Next, source motion needs to be discussed. The DLT study[1] analyzes a closed-loop bearing estimator; in that analysis, source motion is taken into account. One practical effect of substantial source motion is the creation of a need for automatic frequency tracking (AFT). The range term (r_i) provides the information required for the AFT function: Doppler shift is proportional to the time derivative of $r_i(t)$. The present study is cast into a different frame of reference: Two bearing estimators, one closed-loop and the other open-loop, are being compared. To simplify the comparison, source motion is assumed not to exist. Therefore, in this case, the range term (r_i) is constant and conveys no more information than Φ_0 does. Consequently, the AFT function is no longer necessary, hence will receive no further consideration in this report. Furthermore, the input bearing (θ_i) is also constant.

To focus on the informative terms and to eliminate useless terms, attention is now called to the differential phase:

$$\Psi = \Phi_L - \Phi_R \tag{2-5}$$

$$\Psi = \kappa d \ (\sin \theta_i - \sin \theta_o) \tag{2-6}$$

This last equation requires further examination. For a closed-loop bearing estimator the bearing error

$$\theta_e = \theta_i - \theta_o \tag{2-7}$$

will be relatively small if the input signal-to-noise ratio (SNR) is not low, particularly when source motion is absent. For the open-loop bearing estimator, this statement is not necessarily true (this matter will be discussed at greater length in a later section). Again for simplicity the bias, or mean value of θ_e, will be assumed to be zero for the performance comparison. Thus, again if the SNR is reasonable, the bearing error will be small. Under this circumstance (2-6) can be approximated by

$$\Psi \cong (\kappa d \cos \theta_o) \ (\theta_i - \theta_o) \tag{2-8}$$

This expression can be cast into the form

$$\Psi \cong K_{PF} \ (\theta_i - \theta_o) \tag{2-9}$$

where K_{PF} = Horton[5] phase factor:

$$K_{PF} = \kappa d \cos \theta_o \tag{2-10}$$

Equation (2-9) shows that the desired bearing estimate can be obtained from a measurement of differential signal phase. Putting it another way, information concerning bearing is contained in signal phase. Two different ways of extracting this bearing information are described in the next section.

The important fact in all this is that the phase estimate provided by the measurement of differential signal phase is the resultant phase of the signal plus accompanying noise. This aspect is treated in detail in subsequent sections of this report.

3.0 BASIC CONFIGURATIONS

In this section, the basic configurations of the two bearing estimators, whose performance is being compared in this report, are shown and described.

Figure 3-1 shows the closed-loop bearing estimator. Because of familiarity, it is based on the DIFAR-Like Tracker (DLT) analyzed in the DLT study report[1].

The assumed signal waveform and wavefront are as described in the previous section: a sinusoidal signal and a plane wave. The split-array beamformer is also described there.

To minimize the effect of additive noise accompanying the received signal, bandpass filters are used. It is assumed in this report that the received signal lies at the center of the band (f_0). The quantitative effect of the bandwidth (Δf_i) is determined analytically in this report.

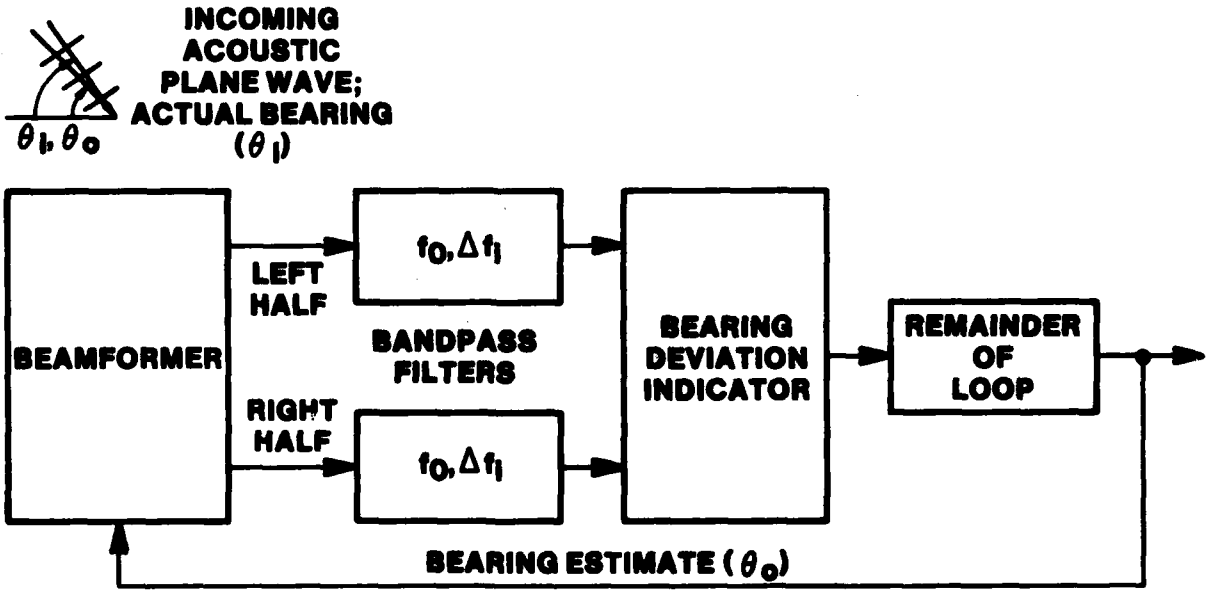

Figure 3-1. Closed-Loop Bearing Estimator

The phase detection function in the DLT closed-loop bearing estimator is performed by a clipper bearing deviation indicator (BDI). More will be said on this subject in the next section.

The remainder of the loop contains the necessary equalizer network for loop stability, and the motor which drives the steering comparator in the beamformer. The output of the motor is the bearing estimate (θ_o), which is driven by the system in such a direction as to minimize the bearing error. The motor provides a single integration, resulting in a Type-I loop. This is all a description of a classical closed-loop feedback system. There is no need to dwell on these matters in this report; all analytical influences are already worked out in the DLT study report[1].

Figure 3-2 shows the basic configuration of the open-loop bearing estimator. The same assumptions are made covering the incoming signal and beamformer, except that the main response axis (MRA) of each beam is now fixed. Probably a set of preformed beams would be used. Actually, no such system can be truly open-loop; at least some kind of loose control is required, if only to select the proper beam and transfer between beams when required. Because of the fixed beam MRA, the information carried in the differential phase is the input bearing rather than bearing error. For the purposes of this report, bearing rate of the signal source is assumed to be zero.

The configuration of Figure 3-2 is based on the use of a commercial spectrum analyzer: the Hewlett-Packard Model HP 3582A. This piece of equipment, it turns out, is inherently capable of performing a number of the required functions of the bearing estimator.

Bandpass filtering is used, as it is in the closed-loop configuration, but this time it is provided by the Fast Fourier Transformation (FFT) contained in the spectrum analyzer. The parameters of a bin are, again, center frequency (f_0) and bandwidth (Δf_1). The dependence of this bandwidth on FFT parameters will be discussed later. The FFT bin output is complex; that is, it appears as a pair of components: in-phase (u) and quadrature (v). There are actually two such pairs in the system, one for the left-hand channel and the other for the right-hand channel.

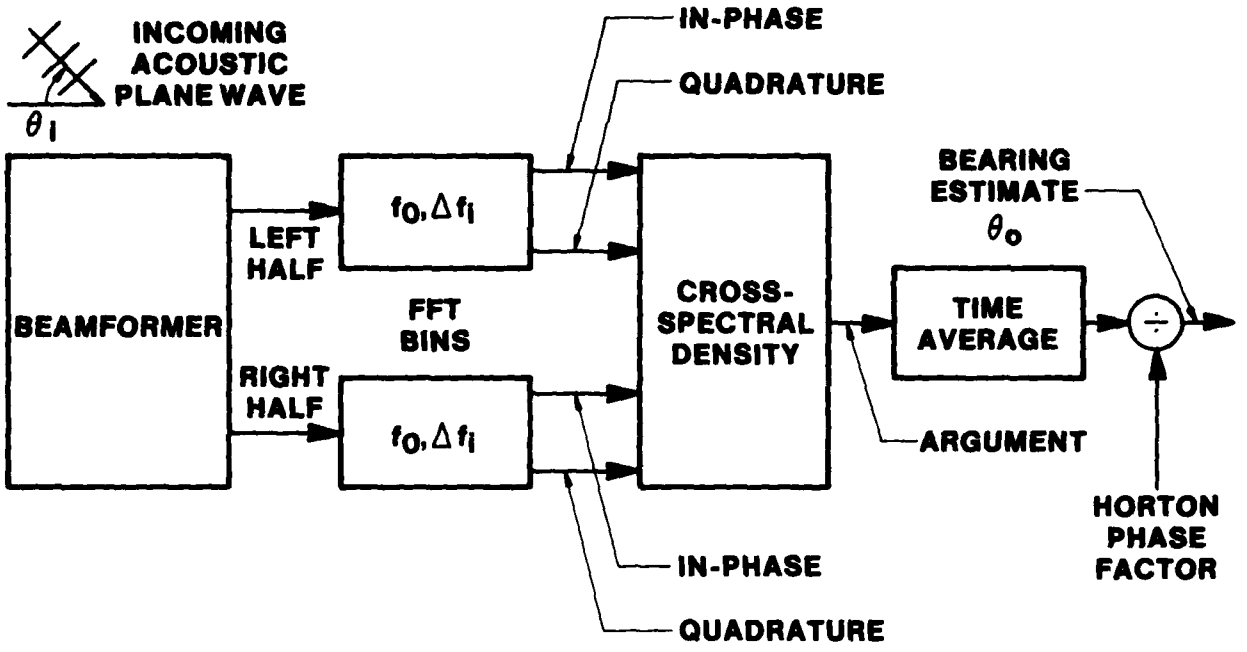

Figure 3-2. Open-Loop Bearing Estimator

The phase-detection function chosen for the open-loop bearing estimator is the argument of the cross-spectral density between the left-half and right-half FFT bin outputs; this is a function contained within the spectrum analyzer. The definition of this quantity is given in the next section.

The phase estimates (ψ) are delivered as a sequence of discrete samples; these samples are averaged arithmetically in the spectrum analyzer. This time averaging is discussed in a later section, and compared with that occurring in the closed-loop bearing estimator.

Finally, the time-averaged phase estimate $\langle\psi\rangle$ is divided by the Horton phase factor to arrive at the bearing estimate:

$$\theta_o = \frac{\langle\psi\rangle}{K_{PF}} \tag{3-1}$$

4.0 PHASE DETECTION

In the previous section, in which the basic configuration of the two bearing estimators is presented, the respective implementations of the phase-detection function appear to be markedly different. Nevertheless, in the present section they are seen to be mathematically identical, with one proviso.

That proviso is that the particular form of the clipper BDI used in the closed-loop bearing estimator be one that employs flip-flops to achieve a sawtooth characteristic spanning all four quadrants; that is, $\pm 180^{\circ}$. Such a circuit can be found in a paper by Lindgren et al[6], for example. When this circuit is used, the resulting output is equal to the differential phase (ψ) between the voltages appearing in the two (left- and right-half) channels, after bandpass filtering. In equation form, these two channel voltages can be expressed in two ways, as follows:

$$A \cos (2\pi f_0 t + \Phi_L) + n_L(t) = C_L \cos (2\pi f_0 t + \phi_L) \tag{4-1}$$

$$A \cos (2\pi f_0 t + \Phi_R) + n_R(t) = C_R \cos (2\pi f_0 t + \phi_R) \tag{4-2}$$

where the left sides are in the form of the sum of a sinusoidal signal with constant amplitude (A) and true phase (Φ), plus Gaussian noise with mean zero and variance (N), statistically independent from channel to channel. The right sides are in the form of a composite voltage with slowly varying envelope (C) and phase (ϕ). The output of a $\pm 180^{\circ}$ BDI, in these terms, will be

$$\psi + 180^{\circ} = (\phi_L - \phi_R + 180^{\circ}) \bmod 360^{\circ} \tag{4-3}$$

defined over

$$-180^{\circ} < \psi \leq +180^{\circ} \tag{4-4}$$

The statistical properties of ψ will be discussed in the following section.

Attention is next turned to the other implementation of the phase-detection function: the argument of the cross-spectral density. This quantity is estimated in the following fashion: The complex coefficients in the two (left- and right-half) FFT bin outputs associated with a particular frequency (f_0) are multiplied,

taking the complex conjugate of one of the outputs prior to multiplication. The cross-spectral density is a complex number; in polar form, its components are a magnitude, which is the commonly used output, and an angle, called the argument, which is used for the present application.

Now the above word procedure will be illustrated mathematically. The FFT bin output components are as follows:

$$u_L = A \cos \Phi_L + n_{L,I} = C_L \cos \phi_L \tag{4-5}$$

$$v_L = A \cos \Phi_L + n_{L,Q} = C_L \cos \phi_L \tag{4-6}$$

$$u_R = A \cos \Phi_R + n_{R,I} = C_R \cos \phi_R \tag{4-7}$$

$$v_R = A \cos \Phi_R + n_{R,Q} = C_R \cos \phi_R \tag{4-8}$$

where the u quantities, and the I subscript, refer to the in-phase components; while the v quantities, and the Q subscript, refer to the quadrature components.

The first operation is the following complex multiplication:

$$(u_L + jv_L)\ (u_R - jv_R) =$$

$$C_L e^{j\phi_L} \quad C_R e^{-j\phi_R} =$$

$$C_L C_R e^{j(\phi_L - \phi_R)} \tag{4-9}$$

The argument (polar angle) of this complex expression is, as implemented in the commercial instrumentation,

$$\psi + 180^0 = (\phi_L - \phi_R + 180^0) \bmod 360^0 \tag{4-10}$$

defined over

$$-180^0 < \psi \leq +180^0 \tag{4-11}$$

which is identical to the $\pm 180^0$ BDI output, given by (4-3) and (4-4).

Thus, the general model for the phase-detection function can be illustrated as in Figure 4-1. The input is (Ψ) the differential phase of the signal, while the output is (ψ) the differential phase of the signal plus noise.

Figure 4-1. Definition of Phase Quantities

5.0 PHASE STATISTICS

In the previous section, the outputs of the phase detectors associated with the closed- and open-loop bearing estimators are shown to be mathematically identical. In the present section, the statistics of this common output are shown. The history and results of the analysis developing these statistics are presented here; the details are given in Appendix A.

An earlier analysis appears in the DLT study report[1]. There the configuration of the well-known clipper BDI, which operates in the first and fourth quadrants of phase--that is, $\pm 90^0$--is shown. A rather detailed analysis is performed in that report to obtain the statistics of the phase estimate provided by this particular circuit. This analysis is based on the probability density function (pdf) of the phase of a sine wave plus Gaussian noise, derived by Middleton in 1948[7]. Later[8], he presented a Fourier series representation of the same pdf. Using this form, and assuming the additive noise terms in the two input channels to be statistically independent of one another, the analysis in the DLT study derives Fourier series expressions for the moments of the differential phase estimate as a function of the input signal-to-noise ratio (SNR) after bandpass filtering.

Now, it was also required in the prosecution of the DLT study to determine the effect on systems performance of employing the other form of clipper BDI, extended to cover all four quandrants ($\pm 180^0$). This is the form considered in the present report. The resulting series are presented in the DLT study report, but the derivation, which is parallel to that presented for the conventional ($\pm 90^0$) BDI, is not shown there.

Another feature of the phase statistics derived in the DLT study is their form. Although the mean and variance of the differential phase estimate (ψ) are both functions of the true differential phase (Ψ), as well as the input SNR, the specific statistics chosen in that study are the slope of the mean curve of ψ versus Ψ evaluated at the origin:

$$\left.\frac{\partial \psi}{\partial \Psi}\right|_{\Psi \to 0}$$

and the standard deviation (square root of the variance) of ψ, also evaluated at Ψ equal to zero.

Thus, in Appendix A of the present report, two additional actions are taken:

a) The derivation of the phase statistics for the extended ($\pm 180^{o}$) BDI is shown explicitly. The work is similar to that by others[9-11]. Because of the mathematical identity of the outputs, these statistics apply also to the argument of the cross-spectral density.

b) The selected statistics are now the mean and standard deviation of the phase estimate (ψ) versus the actual differential phase (Ψ) for various values of SNR.

The results of the derivation in Appendix A are as follows (the units of ψ and Ψ are in radians throughout): The first moment, or mean, of the phase estimate is given by

$$\bar{\psi}(\Psi|z) = 2 \sum_{m=1}^{\infty} \frac{(-1)^{m+1}}{m} B_m^2(z) \sin m\Psi \tag{5-1}$$

The second moment, or mean square, of the phase estimate is given by

$$\overline{\psi^2}(\Psi|z) = \frac{\pi^2}{3} - 4 \sum_{m=1}^{\infty} \frac{(-1)^{m+1}}{m^2} B_m^2(z) \cos m\Psi \tag{5-2}$$

where B_m = coefficient, expressible in various alternative ways, as shown in Appendix A.

The quantity z is defined as

$$a_0^2 = \frac{z}{2} \tag{5-3}$$

where a_0^2 = Middleton's[8] symbol for input signal-to-noise power ratio (SNR).

In terms of system parameters,

$$a_0^2 = \frac{A^2}{2N_0 \Delta f_i} \tag{5-4}$$

where

A = amplitude of sinusoidal signal

N_0 = spectral density of noise (assumed flat over the pass band)

Δf_i = effective noise bandwidth of input bandpass filters.

During the course of the study, it was found that it is quite possible to program the numerical calculation of (5-1) and (5-2), together with the coefficients on a programmable hand calculator: specifically the Hewlett-Packard HP-41C calculator. Three memory modules are required, and the assignment of 150 data registers is sufficient. The calculation is relatively slow, but definitely feasible. The details of the program are being submitted to the Government under separate cover.

Figure 5-1 is a plot of the results of the calculation. The units of the plot are in electrical degrees rather than radians. Shown are the mean and standard deviation (called "SIGMA" in the figure) of the phase estimate (ψ) versus the actual differential phase (Ψ) for several values of SNR in dB.

The features to be noted are as follows: The moments of ψ are expressed in equations (5-1) and (5-2) in Fourier series form, hence are periodic in Ψ. These two equations are derived in Appendix A based on a sawtooth characteristic spanning $\pm 180^0$; thus it can be seen that the period of the moments is 360^0. The mean, given by (5-1), appears as a summation of sine functions, hence is an odd function of Ψ. On the other hand, the standard deviation is an even function of Ψ, for the following reason: In equation form

$$\sigma_\psi(\Psi|z) = \sqrt{\overline{\psi^2}\ (\Psi|z) - \overline{\psi}^2\ (\Psi\ z)} \tag{5-}$$

The first term under the radical is given by (5-2), which appears as a summation o cosine functions, hence is an even function of Ψ. The second term is the square o an odd function, therefore an even function. The difference is even, and so is th positive square root of the difference.

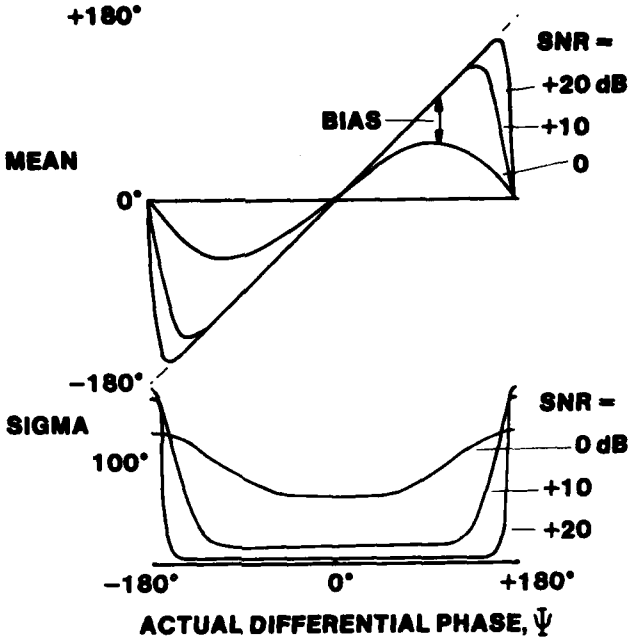

Figure 5-1. Moments of Phase Estimate, ψ

The mean curve has a central linear portion, whose extent is greater when the SNR is higher. The slope of this linear portion, which is important in what follows, is a function of SNR, becoming smaller as SNR decreases. The bias is the difference between the mean of ψ and the true value Ψ; this is shown in the figure. Its value is always zero or negative, because ψ is always less than or equal to Ψ.

The standard deviation curve has a flat central region, whose extent again is greater when the SNR is higher. The value of the standard deviation in this region, which is also important in what follows, is a function of SNR, becoming larger as SNR decreases.

The practical system effects of these attributes of the phase estimation statistics become more clear in following sections of this report.

6.0 LOCATION AND NATURE OF ERROR

Although the two bearing estimators under study in this paper possess phase detection implementations with the same statistics (which are presented in the previous section of this report), there is still a fundamental theoretical difference between the estimators: the location and nature of the error used as a (negative) measure of performance.

In the closed-loop bearing estimator, the bearing error, which is the difference between the output bearing estimate (θ_o) and the input true bearing (θ_i), can be transformed by the Horton phase factor of the beamformer into a corresponding phase error at the input to the phase-detection function; that is, an error in Ψ. In this report, this normalization is in fact made, to eliminate the necessity of specifying operating frequency and aperture size. However, the source of the error is to be found in the output statistics of the phase detection function; that is, the statistics of ψ.

Now, to determine the degree of error in Ψ caused by the statistics of ψ requires a loop analysis; strictly speaking, one that takes into account the nonlinear nature of the phase detection function. Section 4 of the DLT study report[1] presents the history and present state of the art of nonlinear loop analysis. As pointed out there, the use of an analytical technique involving the Focker-Planck equation leads to a probability density function (pdf), thence to the desired moments. In a particularly simple loop configuration (simpler than the DLT loop under consideration here), the result is the Tikhonov[12] distribution:

$$p(\Psi) = \frac{e^{\alpha \cos \Psi}}{2 \pi I_0(\alpha)} \tag{6-1}$$

where

α = the signal-to-noise ratio in the bandwidth of the loop,

I_0 = modified Bessel function of the first kind, zeroth order.

This Tikhonov distribution has a relatively simple appearance, tempting one to make use of it, despite its lack of strict applicability to the DLT loop, as an approximation to account for the large-error domain. In the end, however, the decision has been made to resort once again to the linearized loop analysis used in the DLT study. (In making such a decision, it is necessary to be aware at the outset that a linearized analysis does not speak to the problems of acquisition and cycle slipping.)

In the linearized analysis, the slope of the central linear portion of the mean of ψ is regarded as the gain factor of the phase detector. The symbol (K_{PD}) will be used in this report, although the quantity so defined differs from that with the same symbol in the DLT study report by a factor of π for the $\pm 180^{\circ}$ BDI. The definition in the present report is

$$K_{PD} = \left. \frac{\partial \overline{\psi}}{\partial \Psi} \right|_{\Psi \to 0} \tag{6-2}$$

When this is done, the normal action of the closed feedback loop is to yield the following equation[1]:

$$\sigma_{\Psi} = \frac{\sigma_{\psi}(0|z)}{K_{PD}} \sqrt{\frac{\Delta f_e}{\Delta f_i/2}} \tag{6-3}$$

where

Δf_e = effective noise bandwidth of the closed loop,

Δf_i = effective noise bandwidth of the input bandpass filters.

The other factors have already been defined in this report.

At this point, it is well to mention that, in the absence of a bearing rate, the closed-loop bearing estimator produces an unbiased estimate. Put another way, this Type-I loop (single integration) produces no lag error in the absence of a bearing rate.

Turning to the open-loop bearing estimator, the output bearing estimate (θ_o) is given by

$$\theta_o = \frac{\langle \psi \rangle}{K_{PF}} \tag{6-4}$$

where

$\langle\ \rangle$ = arithmetic average over K samples,

K_{PF} = Horton phase factor, defined earlier.

As before, normalization is applied by removing the Horton phase factor, so that operating frequency and aperture size need not be specified. The quantity to be studied becomes simply $\langle \psi \rangle$, the time-averaged phase at the output of the phase detector. The phase estimate at the output of the phase detector is in general biased. in the previous section, the mean ($\bar{\psi}$) is plotted versus the true phase (Ψ) for various values of SNR. It can be seen that there is a difference between $\bar{\psi}$ and Ψ (that is, a bias) for nonzero Ψ and finite SNR. The time-averaging process will reduce the standard deviation of the estimate, but will not affect the bias.

For the purpose of the performance comparison in this report, the question of bias will be ignored. It is assumed that the sound source is on the beam main response axis (MRA), so that the actual differential phase (Ψ) is zero. Figure 5-1 shows that this results in the mean phase estimate (ψ) going to zero, independent of SNR; hence the bias, which is the difference between ψ and Ψ, is also zero.

Having assumed away the bias, the expression for error is in terms of the standard deviation:

$$\sigma_{\langle \psi \rangle} = \frac{\sigma_\psi(0|z)}{\sqrt{K}} \tag{6-5}$$

Equation (6-3) predicts the theoretical performance of the closed-loop bearing estimator, while equation (6-5) does the same for the open-loop bearing estimator. Now, these two equations are difficult to interpret and compare in their present forms. Therefore, they will be manipulated further in the next section.

7.0 COMPARATIVE PERFORMANCE

In this section, the final performance expression will be developed and the results of a numerical evaluation of these expressions will be plotted to show the comparative performance of the closed- and open-loop bearing estimators.

Both preliminary performance equations, (6-3) and (6-5), include the idea of the reduction of fluctuations by time-averaging over a fixed time interval called the observation time, which can be called T_{obs}. The resulting standard deviation in each case is inversely proportional to the square root of T_{obs}. For further universality of the results, it is possible to eliminate the necessity of specifying a value for this observation time by evaluating the product of the standard deviation and the square root of T_{obs}. This idea is not original with this report; Fischer[13] employed it in an earlier comparative study.

The closed-loop bearing estimator is taken up first. Multiplying (6-3) by the square root of the observation time yields the following:

$$\sigma_\Psi \sqrt{T_{obs}} = \frac{\sigma_\psi(0|z)}{K_{PD}} \sqrt{\frac{2\Delta f_e T_{obs}}{\Delta f_i}} \tag{7-1}$$

The following rule of thumb is suggested, relating the equivalent observation time to the effective noise bandwidth of the analog loop:

$$T_{obs} = \frac{1}{2\Delta f_e} \tag{7-2}$$

During the course of this study, the validity of (7-2) has been tested empirically using real data from the DLT Engineering System Test Model (ESTM).

On the theoretical side, the effective noise bandwidth is computed for the specific system used for taking the data in question by making use of the equation[1]

$$\Delta f_e = \frac{K_v^{0.7}}{4T^{0.3}} \tag{7-3}$$

where

K_v = the analog loop gain constant, sometimes called the velocity error constant, in units of reciprocal seconds

T = the (effective) largest open loop time constant, in seconds.

Without specifically reporting the system parameters, the numerical value of the effective noise bandwidth comes out to be 0.032 Hz in one particular case, resulting in an observation time, using (7-2), of 15.6 seconds.

On the empirical side, the computed autocorrelation function of the real DLT ESTM output data is shown in Figure 7-1. It will be noted that the autocorrelation function first reaches zero--signaling statistical independence--at a lag of 17 seconds. Equating this time between independent samples to the desired observation time, the agreement is not bad.

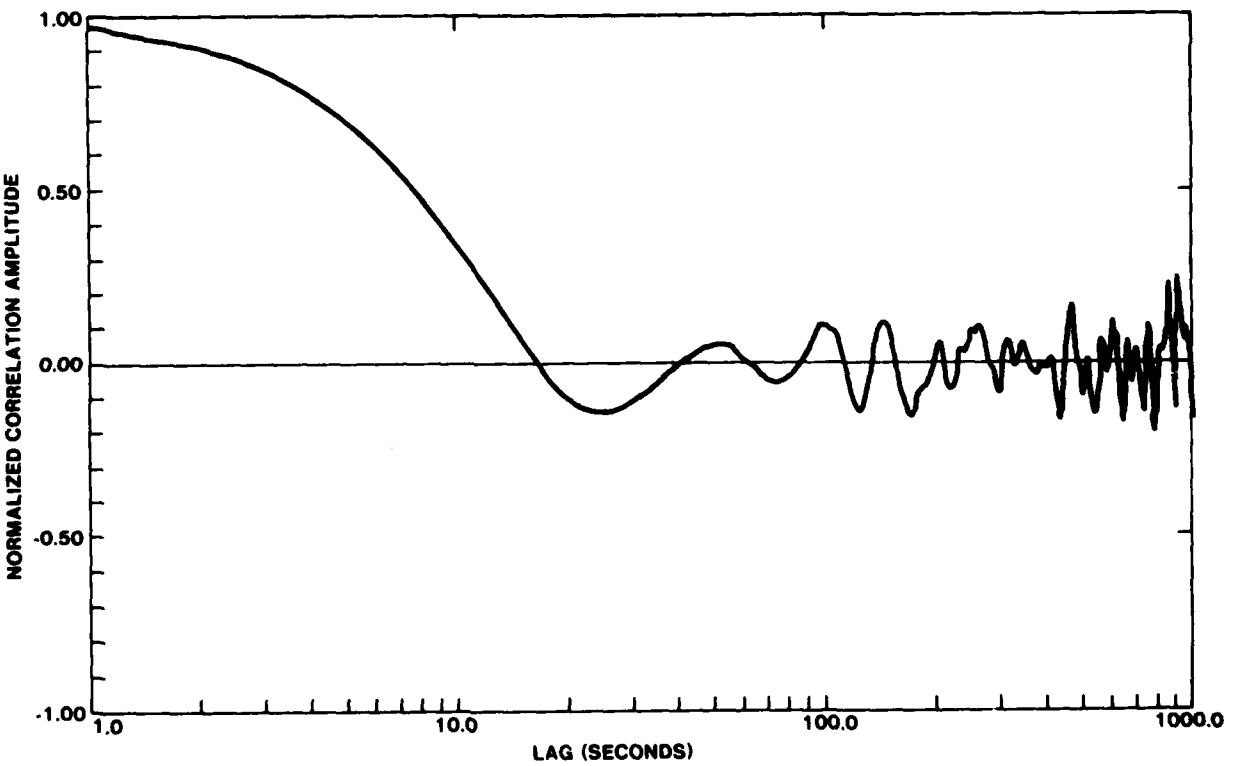

Figure 7-1. Autocorrelation Function of DLT ESTM Data

Substituting (7-2) into (7-1) yields

$$\sigma_\Psi \sqrt{T_{obs}} = \frac{\sigma_\psi(0|z)}{K_{PD}} \sqrt{\frac{1}{\Delta f_i}} \tag{7-4}$$

Next, attention is turned to the open-loop bearing estimator. Equation (6-5), repeated here for convenience,

$$\sigma_{\langle\psi\rangle} = \frac{\sigma_\psi(0|z)}{\sqrt{K}} \tag{6-5}$$

is written in terms of the quantity K, the number of samples of ψ entering the time averaging process. There is implicit in (6-5) the assumption of statistically independent samples. This matter deserves further discussion.

In the first place, the samples in question are taken from an FFT bin, the input to which is a sequence of input data of time duration T_{fft}. Now, a process called "overlapping" is sometimes used, wherein the first, say fifty percent, of the input sequence associated with one output sample is identical to the last fifty percent of the input sequence associated with the previous output sample. In such a case, the output samples would be correlated with each other. Such overlapping is not intended in the open-loop bearing estimator, and is not provided in the HP-3582A spectrum analyzer.

In the absence of overlapping, the output samples tend to be uncorrelated with each other to a large degree, particularly if a large number of input samples (for example, 1024) is used in the input sequence. There may be a small "edge effect" representing the correlation between input samples at the beginning of one sequence and input samples at the end of the previous sequence. This effect should be quite negligible in practice.

Thus the expression for the number K is simply

$$K = \frac{T_{obs}}{T_{fft}} \tag{7-5}$$

Therefore

$$\sigma_{\langle\psi\rangle}\sqrt{T_{obs}} = \sigma_{\psi}(0|z)\ \sqrt{T_{fft}} \tag{7-6}$$

In order to have a common basis for performance comparison, it would be desirable to write (7-6) in terms of the input bandwidth, Δf_i. This bandwidth has been specified as the effective noise bandwidth of the input bandpass filter, in this case the FFT bin.

Harris[14] has published a comprehensive treatment of the quantitative effect of "window" shape on a number of FFT parameters, including effective noise bandwidth. A window is a time-domain weighting function used to improve the qualities of the spectral estimates. The effective noise bandwidth can be expressed as follows:

$$\Delta f_i = \frac{\mu}{T_{fft}} \tag{7-7}$$

where μ = a constant whose numerical value depends on the exact window shape (tabulated in the fifth column of Table I in Harris[14]).

Substituting (7-7) into (7-6),

$$\sigma_{\langle\psi\rangle}\sqrt{T_{obs}} = \sigma_{\psi}(0|z)\ \frac{\mu}{\Delta f_i} \tag{7-8}$$

Rather than letting the estimator comparison become bogged down in FFT details, the decision is made at this point to assume a Dirichlet window, which is simply constant over the time interval of length T_{fft}, zero otherwise (in other words, a rectangular window). For this window,

$\mu = 1$,

resulting in

$$\sigma_{\langle\psi\rangle}\sqrt{T_{obs}} = \frac{\sigma_{\psi}(0|z)}{\sqrt{\Delta f_i}} \tag{7-9}$$

All that remains for a performance comparison is a numerical evaluation of (7-4) for the closed-loop bearing estimator and (7-9) for the open-loop bearing estimator. The right-hand sides of the two equations are identical, except for the phase detector gain factor (K_{PD}). They both require the standard deviation of the phase estimate given by (5-6) evaluated where the true differential phase (Ψ) is zero. In addition, the quantity (K_{PD}), given by (6-2), is expressed in series form and evaluated for use in (7-4). The quantity is also evaluated in the DLT study report[1], but differs from the corresponding quantity in the present report by a factor of π, because of definition.

Figure 7-2 is a plot of the results of the above-described calculation. The appropriate normalized phase error used as a (negative) measure of performance in this report is plotted versus signal-to-noise ratio in the half beam and in a 1-Hz band, this latter for further universality of the results. In decibels, the abscissa is

$$10 \log \frac{A^2}{2N_0}$$

The input bandwidth (Δf_i) appears as a parameter of these curves.

By inspection of Figure 7-2, it can be seen that the performance of the two bearing estimators is different at low signal-to-noise ratios, because of the presence of the phase detector gain factor in the closed-loop expression (7-4). This factor causes the phase error to increase as the signal-to-noise ratio decreases. Physically, this increase can go on only so far before track is broken and cycle-slipping occurs, a phenomenon not considered explicitly in this report. As mentioned earlier, a different and more involved analytical procedure is required to account for this phenomenon. If such a procedure were to be used, probably the curves would be more similar to each other in this low SNR region.

The phase error for the open-loop estimator, on the other hand, can be seen to approach a constant asymptote, whose value depends on the input bandwidth (Δf_i), as the SNR decreases. The asymptotic value is that associated with the uniform phase distribution characteristic of pure Gaussian noise.

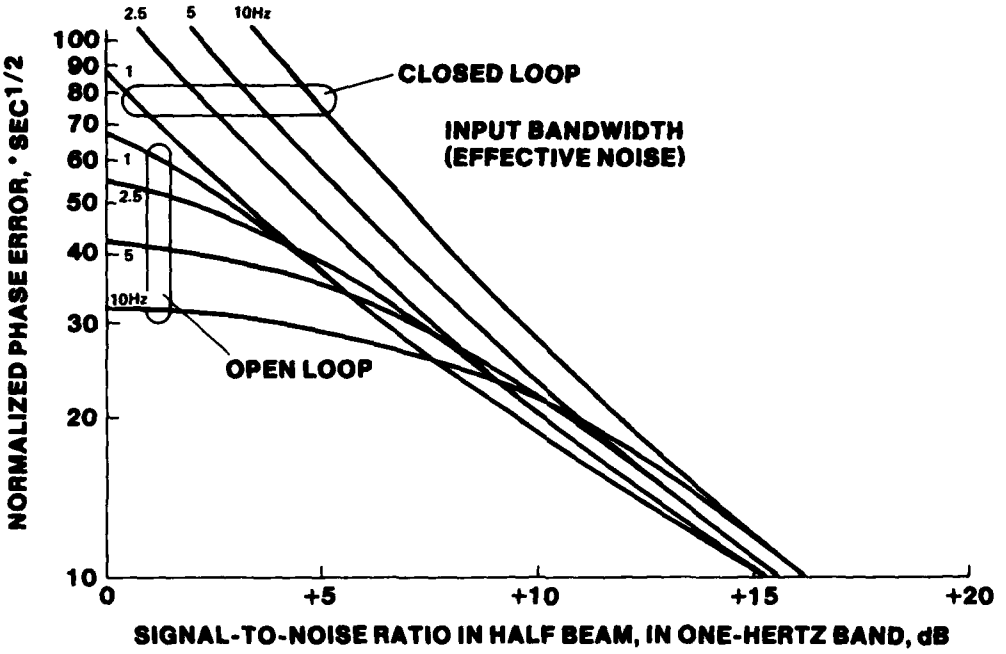

Figure 7-2. Comparative Performance

The important conclusion of the paper is arrived at by an examination of the performance curves at high signal-to-noise ratios. It can be seen that all curves approach each other, and the performance, defined as it is in this paper, becomes independent of input bandwidth, but, more importantly, becomes the same for the closed-loop and open-loop bearing estimators.

Thus, the decision as to which of the two estimator concepts to use should be based on practical implementation considerations rather than theoretical performance. Operational system studies will, of course, need to address the question of source motion and statistical estimate bias deliberately excluded from consideration in this report.

8.0 REFERENCES

1. Bartram, J.F., and J.I. Salisbury, Technical Report: DIFAR-Like Bearing Tracking Study (U), Raytheon Co., Submarine Signal Division, January 1975 (Confidential).

2. Final Report: Analysis of a Post-Detection Automatic Target Following Technique for Multi-Beam Receiving Systems, Raytheon Co., October 1964 (Declassified).

3. Bartram, J.F., "Preformed Beam Interpolation for Bearing Estimation," Raytheon Co., Submarine Signal Division Internal Memorandum JFB: 74/25, 20 June 1974.

4. Jarvis, H.F. Jr., "Beam Amplitude Interpolation Tracking Using Closed-Loop Methodology," Analysis & Technology, Inc., August 1981.

5. Horton, J.W., Fundamentals of Sonar, United States Naval Institute, Annapolis, Maryland, 1959.

6. Lindgren, A.G., R.F. Pinkos, and R.H. Berube, "Noise Dynamics of the Phase-Locked Loop with Signal Clipping," IEEE Trans. on Aerosp. and Electron. Syst. Vol. AES-5, January 1964, pp 66-76.

7. Middleton, D., "Some General Results in the Theory of Noise through Non-Linear Devices," Quart. Appl. Math., Vol. 5, 1948, pp 445-498, Equation 5.16.

8. Middleton, D., Introduction to Statistical Communication Theory, McGraw-Hill, New York, 1960, Equation 9.58.

9. Callahan, A.C., "On Phase Difference Estimators," Raytheon Submarine Signal Division, Internal Memorandum ACC: 75/14, 16 September 1975.

10. Jarvis, H.F. Jr. and D.B. Cretella, "Quasi-Linear Analysis of Conventional and IQ-Locked Loop Trackers (U)," Analysis & Technology, Inc., 23 November 1979.

11. Raab, F.H., "Low-Frequency Correlation Phase Detection Using Hard Limiting," IEEE Trans. on Aerosp. Electron. Syst., Vol. AES-17, March 1981, pp 305-311.

12. Tikhonov, V.I., "The Effects of Noise on Phase-Lock Oscillation Operation," Automatika i Telemekhanika, Vol. 22, no. 9, 1959; translated in Automation and Remote Control, Vol. 20, no. 9, September 1959, p 1160.

13. Fischer, W.K., DIFAR-Like Bearing Tracker Performance Comparison (U), TD-111-C20-76, NUSC/NLL, 12 May 1976 (Confidential Report).

14. Harris, F.J., "On the Use of Windows for Harmonic Analysis with the Discrete Fourier Transform," Proc. IEEE, Vol. 66, no. 1, January 1978, pp 51-83.

15. Jolley, L.B.W., Summation of Series, Second revised edition, Dover Publications, Inc., New York, 1961.

16. Handbook of Mathematical Functions, National Bureau of Standards, Applied Mathematics Series 55, June 1964.

17. Random Bearing Error Analysis, Sonalysts, Inc., 25 February 1980.

18. "Signal Averaging with the HP 3582A Spectrum Anayzer," Application Note 245-1, Hewlett-Packard Co. (undated).

APPENDIX A

DERIVATION OF PHASE STATISTICS

In this appendix, the statistics of the estimate of differential phase provided by the phase-detection function of the two bearing estimators of this report will be derived. In the main text it is shown that the two phase-detection implementations, while outwardly quite different, provide mathematically identical phase estimates. Also, it turns out that much of the derivation has already been given in Section 6.8 of the DLT study report[1]. In addition, others[9-11] have published similar results.

The specific quantities derived here are:

a) Mean of the differential phase estimate as a function of the true differential phase, and input signal-to-noise ratio.

b) Standard deviation of the differential phase estimate as a function of the true differential phase, and input signal-to-noise ratio.

c) First derivative (slope) of the phase estimate mean with respect to the true differential phase, evaluated where the latter independent variable is zero, versus input signal-to-noise ratio. This quantity is called the phase-detector gain factor in this report (with a caveat about its scale factor).

The derivation starts with the expression for the ν^{th} moment of the differential phase estimate:

$$\overline{\psi^{\nu}}\,(\Phi_L,\Phi_R;z) = \int_{-\pi}^{+\pi}\int_{-\pi}^{+\pi} \psi^{\nu}(\phi_L - \phi_R)\quad p(\phi_L \mid \Phi_L;z)\cdot p(\phi_R \mid \Phi_R;z)\; d\phi_L\, d\phi_R \tag{A-1}$$

where

ψ = differential phase estimate

$\phi_{L,R}$ = phase of the signal-plus-noise voltage in the (left, right) channel

$\Phi_{L,R}$ = phase of the signal in the absence of noise (true phase) in the (left, right) channel

$p(\phi|\Phi;z)$ = conditional probability density function (pdf) of ϕ, given values of Φ and z (defined below)

z = input signal-to-noise ratio (not in dB), divided by 2.

At this point it is well to point out that the form of (A-1) with the product of two pdf factors appearing, implies that the noises in the two (left and right) channels are statistically independent of each other. This is a common assumption in studies of this type, although it is recommended that this assumption be relaxed in any follow-on studies.

There is more to the story than independence, however. The fact that the two pdf factors appear without subscripts implies that they are functionally identical. Also the same value of the parameter z appears in both factors, indicating an identical input signal-to-noise ratio (SNR) existing in both channels. The DLT study report[1] went into the question of unequal SNR values, but the present study does not.

The next step is to specify the functional form of ψ. In the main text, the following is established for both phase detector implementations:

$$\psi + 180^\circ = (\phi_L - \phi_R + 180^\circ) \bmod 360^\circ \qquad \text{(A-2)}$$

This rather compact algebraic expression describes the periodic sawtooth characteristic pictured in Figure A-1. This figure resembles Figure 6-4b of the DLT study report[1], but the vertical axis has a different scale factor.

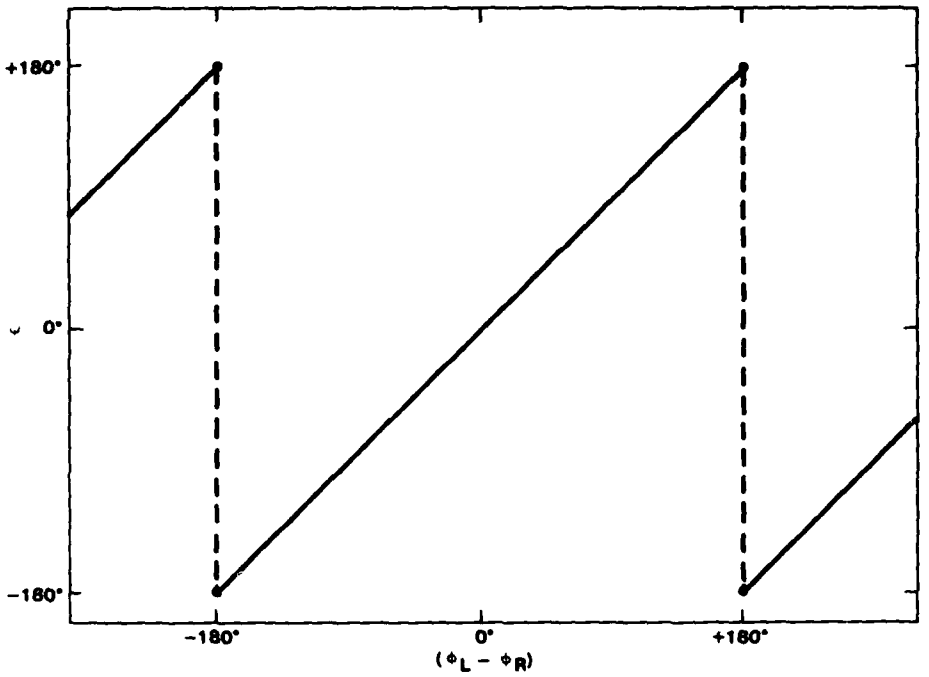

Figure A-1. Sawtooth Characteristic

Equation (A-2) cannot be used in (A-1) in its present form. Since the probability density function (p) will be seen to be expressible in Fourier series form, it will be mathematically convenient to express ψ in the same way. Because the function is periodic, this form is quite appropriate and natural.

Formula (509) of Jolley[15] furnishes the required series, after some elementary manipulation:

$$\psi = 2 \sum_{m=1}^{\infty} \frac{(-1)^{m+1}}{m} \sin m(\phi_L - \phi_R) \qquad \text{(A-3)}$$

It will be noted that this series is not the same as (6-58) of the DLT study report[1]. The latter series applies to the triangular, or $\pm 90°$, characteristic of Figure 6-4a instead.

Now, a series for ψ is not enough; one is required for ψ^2 as well. Again, Jolley furnishes the required series, this time in Formula (517), after some elementary manipulation:

$$\psi^2 = \frac{\pi^2}{3} - 4 \sum_{m=1}^{\infty} \frac{(-1)^{m+1}}{m^2} \cos m(\phi_L - \phi_R) \tag{A-4}$$

Now, (A-3) and (A-4) are written in terms of the difference between ϕ_L and ϕ_R separately. It will therefore be convenient to rewrite (A-3) and (A-4) in a similar fashion, through the use of trigonometric identities:

$$\begin{aligned} \psi = 2 &\sum_{m=1}^{\infty} \frac{(-1)^{m+1}}{m} \sin m\phi_L \cos m\phi_R \\ -2 &\sum_{m=1}^{\infty} \frac{(-1)^{m+1}}{m} \cos m\phi_L \sin m\phi_R \end{aligned} \tag{A-5}$$

$$\begin{aligned} \psi^2 = \frac{\pi^2}{3} - 4 &\sum_{m=1}^{\infty} \frac{(-1)^{m+1}}{m^2} \cos m\phi_L \cos m\phi_R \\ + 4 &\sum_{m=1}^{\infty} \frac{(-1)^{m+1}}{m^2} \sin m\phi_L \sin m\phi_R \end{aligned} \tag{A-6}$$

It is now possible to substitute (A-5) and (A-6) into (A-1), interchanging the summations and integrations, which is legitimate here:

$$\begin{aligned} \overline{\psi} = 2 &\sum_{m=1}^{\infty} \frac{(-1)^{m+1}}{m} \overline{\sin m\phi_L} \; \overline{\cos m\phi_R} \\ -2 &\sum_{m=1}^{\infty} \frac{(-1)^{m+1}}{m} \overline{\cos m\phi_L} \; \overline{\sin m\phi_R} \end{aligned} \tag{A-7}$$

$$\begin{aligned} \overline{\psi^2} = \frac{\pi^2}{3} - 4 &\sum_{m=1}^{\infty} \frac{(-1)^{m+1}}{m^2} \overline{\cos m\phi_L} \; \overline{\cos m\phi_R} \\ + 4 &\sum_{m=1}^{\infty} \frac{(-1)^{m+1}}{m^2} \overline{\sin m\phi_L} \; \overline{\sin m\phi_R} \end{aligned} \tag{A-8}$$

where

$$\overline{\sin m\phi} \equiv \int_{-\pi}^{+\pi} p(\phi|\Phi;z) \sin m\phi \, d\phi \tag{A-9}$$

$$\overline{\cos m\phi} \equiv \int_{-\pi}^{+\pi} p(\phi|\Phi;z) \cos m\phi \, d\phi \tag{A-10}$$

The specific expression for (p), the probability density function of the phase of a sinusoid plus Gaussian noise, is available, having been derived by Middleton[7,8]. It is not necessary, however, to write the expression explicitly, since the results of the integrations in (A-9) and (A-10) also have been given by Middleton[8]:

$$\overline{\sin m\phi} = B_m(z) \sin m\Phi \tag{A-11}$$

$$\overline{\cos m\phi} = B_m(z) \cos m\Phi \tag{A-12}$$

where

$$B_m = \frac{a_0^m}{m!} \Gamma\left(\frac{m}{2} + 1\right) {}_1F_1\left(\frac{m}{2}; m + 1; -a_0^2\right) \tag{A-13}$$

where, in turn,

a_0^2 = input signal-to-noise ratio (not in dB). This is related to z by the relationship $a_0^2 = z/2$.

$\Gamma(\,)$ = gamma function

${}_1F_1$ = confluent hypergeometric function

The functions will be related to other, somewhat simpler, functions later.

Now, (A-11) and (A-12) can be substituted into (A-7) and (A-8):

$$\bar{\psi} = 2 \sum_{m=1}^{\infty} \frac{(-1)^{m+1}}{m} B_m^2(z) \sin m\Phi_L \cos m\Phi_R$$

$$-2 \sum_{m=1}^{\infty} \frac{(-1)^{m+1}}{m} B_m^2(z) \cos m\Phi_L \sin m\Phi_R \qquad \text{(A-14)}$$

$$\overline{\psi^2} = \frac{\pi^2}{3} - 4 \sum_{m=1}^{\infty} \frac{(-1)^{m+1}}{m^2} B_m^2(z) \cos m\Phi_L \cos m\Phi_R$$

$$+4 \sum_{m=1}^{\infty} \frac{(-1)^{m+1}}{m^2} B_m^2(z) \sin m\Phi_L \sin m\Phi_R \qquad \text{(A-15)}$$

Using the trigonometric identities in reverse,

$$\bar{\psi} = 2 \sum_{m=1}^{\infty} \frac{(-1)^{m+1}}{m} B_m^2(z) \sin m\Psi \qquad \text{(A-16)}$$

$$\overline{\psi^2} = \frac{\pi^2}{3} - 4 \sum_{m=1}^{\infty} \frac{(-1)^{m+1}}{m^2} B_m^2(z) \cos m\Psi \qquad \text{(A-17)}$$

where

$$\Psi \equiv \Phi_L - \Phi_R \qquad \text{(A-18)}$$

The following quantities have been calculated numerically in this report:

$$\psi(\Psi|z)$$

$$\sigma_\psi(\Psi|z) =$$

$$\overline{\psi^2} - \bar{\psi}^2$$

$$K_{PD}(z) = \left.\frac{\partial \bar{\psi}}{\partial \Psi}\right|_{\Psi \to 0}$$

This last quantity, called the phase detector gain, differs from the quantity by the same name in the DLT study report by a scale factor of π. In the present report, the specific expression is

$$K_{PD} = 2 \sum_{m=1}^{\infty} (-1)^{m+1} B_m^2 \quad (z) \qquad \text{(A-19)}$$

Earlier in this appendix, it was mentioned that alternative forms exist for the expression (A-13) for the coefficient B_m. The confluent hypergeometric function can be expressed in terms of the Bessel function, with the following result:

$$B_m = \sqrt{\frac{\pi z}{2}}\, e^{-z} \left[I_{\frac{m-1}{2}} (z) + I_{\frac{m+1}{2}} (z) \right] \qquad \text{(A-20)}$$

where I_n ( ) = modified Bessel function of order n.

For numerical calculations, there exist convenient recursive relationships for calculating all the Bessel functions, hence all the coefficients (B_m) in terms of the following basic functions:

I_0 and I_1

$I_{1/2}$ and $I_{3/2}$

The values for (I_0) and (I_1) can be calculated using equations 9.8.1 through 9.8.4 of the National Bureau of Standards handbook[16]. There is a sufficient number of registers in the HP-41C calculator, with three memory modules installed, to have the necessary coefficients for the NBS equations prestored.

The other, fractional order, modified Bessel functions, ($I_{1/2}$) and ($I_{3/2}$) are expressible in terms of the simple exponential function, which is provided in the calculator.

As already mentioned, the details of the program to carry out the recursive relationships to evaluate the coefficients, and the subsequent summation of the series, are being provided to the Government under separate cover.

APPENDIX B

DIFFERENTIAL PHASE vs INDIVIDUAL PHASE

Early in this study, it was recognized that it is necessary to have phase statistics in order to predict system performance. Prior to the theoretical development of Appendix A and the subsequent numerical calculation, the idea was conceived of obtaining phase statistics by a Monte Carlo computer simulation.

Such a simulation was in fact performed, initially by NUSC New London Laboratory, and then completed by Sonalysts, Inc[17]. The specific task was aimed at comparing three different averaging techniques:

$$\text{I.} \quad \langle\phi\rangle = \tan^{-1} \frac{\langle u \rangle}{\langle v \rangle}$$

$$\text{II.} \quad \langle\phi\rangle = \left\langle \tan^{-1} \frac{u}{v} \right\rangle$$

$$\text{III.} \quad \langle\phi\rangle = \tan^{-1} \left\langle \frac{u}{v} \right\rangle$$

where the corner brackets signify a simple arithmetic average over a finite number (K) of independent samples. Several statements can be made about this study of time-averaging techniques:

a) The full details appear in the Sonalysts report[17].

b) In that report, it is found that Technique III is inadequate. The reasoning is given there.

c) For the same amount of averaging (number of independent samples), Techniques I and II are comparable at high signal-to-noise ratios (SNR), but Technique II is superior at low SNR where the phase distributions approach the uniform distribution characteristic of Gaussian noise alone.

d) In fact, the selected bearing estimator configurations utilize Technique II. For the HP3582A spectrum analyzer see Reference 18.

Now, having performed the Monte Carlo simulation, it seemed that the results could then be used for the comparative performance predictions for the open- and closed-loop bearing estimators.

The first fact to be noted is that the Monte Carlo simulation was of the phase of a sinusoid plus Gaussian noise; in other words, the phase in one channel. The phase detectors in the bearing estimators provide an estimate of differential phase between two channels. It is thus necessary, if the Monte Carlo simulation results are to be used for performance prediction, to relate the statistics of differential phase to those of individual phase.

The initial (mistaken) theory was as follows: The differential phase estimate provided by the two phase detectors was assumed to be

$$\psi = \phi_L - \phi_R, \tag{B-1}$$

a simple subtraction. If (B-1) were true, the mean and variance would be as follows:

$$\bar{\psi} = \bar{\phi}(\Phi_L; \text{SNR}) - \bar{\phi}(\Phi_R; \text{SNR}) \tag{B-2}$$

$$\sigma_\psi^2 = \sigma_\phi^2(\Phi_L; \text{SNR}) + \sigma_\phi^2(\Phi_R; \text{SNR}) \tag{B-3}$$

If

$$\Phi_L = -\Phi_R = \Phi$$

$$\Psi = \Phi_L - \Phi_R = 2\Phi$$

$$\bar{\psi} = 2\bar{\phi}(\Psi/2; \text{SNR}) \tag{B-4}$$

and

$$\sigma_\psi^2 = 2\sigma_\phi^2(\Psi/2; \text{SNR}) \tag{B-5}$$

Equations (B-4) and (B-5) would provide the required relationship between the statistics of the differential phase on the one hand and individual phase on the other, if (B-1) were true. Unfortunately, however, (B-1) is not true.

It has been established in the main text that the correct expression for the differential phase estimate provided by the phase detectors in the two bearing estimators is as follows:

$$\psi + 180^\circ = (\phi_L - \phi_R + 180^\circ) \bmod 360^\circ \qquad \text{(B-6)}$$

where the 180° term centers the domain of definition about zero, and the mod 360° operation causes the domain to extend over all four quadrants (360°):

$$-180^\circ < \psi \leq +180^\circ$$

The difference between the correct expression (B-6) and the simpler expression (B-1) resides in a phenomenon called "phase wraparound".

The correct differential phase statistics are those derived in Appendix A. The statistics are related to those of individual phase in a simple fashion only when true phase is near zero and the signal-to-noise ratio is high; these conditions ensuring a low probability of "wraparound".

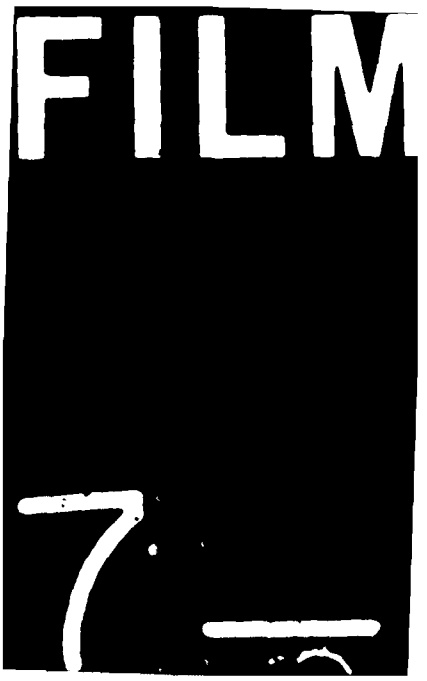
FILM